Pictorial Essay
pISSN 1738-2637 / eISSN 2288-2928
J Korean Soc Radiol 2018;78(3):200-211
https://doi.org/10.3348/jksr.2018.78.3.200

대한영상의학회지

Lesions that Mimic Musculoskeletal Infection: A Pictorial Essay
근골격계 감염과 유사한 질환들: 임상 화보

Hye Jin Kang, MD[1], Hee Young Choi, MD[1], Ji Seon Park, MD[1], So Young Park, MD[2], Wook Jin, MD[2], Kyung Nam Ryu, MD[1]*

[1]Department of Radiology, Kyung Hee University Hospital, College of Medicine, Kyung Hee University, Seoul, Korea
[2]Department of Radiology, Kyung Hee University Hospital at Gangdong, College of Medicine, Kyung Hee University, Seoul, Korea

Musculoskeletal (MSK) infections, such as osteomyelitis, infectious arthritis and spondylitis have variable radiographic findings depending on their underlying cause and clinical infection stage. Other disease entities, ranging from simple degenerative lesions to tumorous bone conditions, in which there is no evidence of infectious origin, can share similar radiographic findings. It is important to be aware, when interpreting radiographic features that are typically associated with MSK infections, that a non-infectious MSK disease may be mimicking the radiographic findings of infectious diseases.

Index terms
Osteomyelitis
Infectious Arthritis
Magnetic Resonance Imaging

Received August 14, 2017
Revised October 3, 2017
Accepted November 11, 2017
***Corresponding author:** Kyung Nam Ryu, MD
Department of Radiology, Kyung Hee University Hospital, College of Medicine, Kyung Hee University, 23 Kyungheedae-ro, Dongdaemun-gu, Seoul 02447, Korea.
Tel. 82-2-958-8617 Fax. 82-2-968-0787
E-mail: t2star@naver.com

INTRODUCTION

Musculoskeletal (MSK) infections can cause a range of symptoms from simple joint pain to serious, debilitating conditions, such as sepsis and physical disability. Despite improvements in personal hygiene, the discovery of antibiotics, and advancements in surgical treatments, MSK infectious diseases are still frequently encountered in clinical practice. Early and accurate diagnosis is critical for the best possible outcomes from therapy. However, diagnosing MSK infections is not always straightforward and often requires a process of differential diagnosis among multiple non-infectious disease entities (1). Various diagnostic imaging techniques, as well as clinical and laboratory records, are used in combination to prevent misdiagnosis. However, a variety of MSK diseases can mimic infection both radiologically and clinically. For example, atypical manifestations of common bone tumors such as osteosarcoma and histiocytosis may present with cortical destruction, periosteal reaction, and adjacent soft tissue swelling, which are all also typical of MSK infections.

In this review article, we discuss three infectious MSK diseases that are considered most important in clinical practice: osteomyelitis, infectious arthritis, and infectious spondylitis. Osteomyelitis is categorized into three clinical stages (acute, subacute, and chronic) because each stage has its own distinctive imaging features. Typical radiographic characteristics of each disease category are presented, followed by mimicking cases.

ACUTE OSTEOMYELITIS

Osteomyelitis is an inflammation of bone and bone marrow caused by an infecting organism. When the infection develops within the first 14 days following an initiating event, such as an injury, or the start of an underlying disease, it is clinically classified as acute osteomyelitis (2). On plain radiographs and CT scans, permeative bone destruction, indistinctiveness of the

cortex, and periosteal reaction are frequently observed in acute osteomyelitis cases.

Permeative Bone Destruction and Periosteal Reaction

The earliest osseous change observed in acute osteomyelitis is indistinctiveness of the cortex, followed by spotty, mottled rarefaction, usually on the metaphyses of long bones (3). Periosteal thickening and new bone apposition are the most common subsequent changes (4). Yet such findings are not specific to acute osteomyelitis. The following is an example of a mimic.

The proximal humerus of a 10-year-old female patient showed extensive bone destruction with "moth-eaten" and permeative patterns on plain radiographs (Fig. 1A). The bony lesion was located on the terminal metaphysis, on which discontinuous periosteal reactions were also visible. On MRI scans taken for further evaluation, soft tissue adjacent to the osteolytic bony lesion showed strong enhancement in contrast-enhanced view, suggesting the presence of inflammation (Fig. 1B). All these imaging appearances led to an initial suspected diagnosis of acute osteomyelitis. However, this case was confirmed to be an osteosarcoma. It is important to remember that permeative, destructive bony lesions with peritumoral edema are also typical of radiographic findings seen in osteosarcoma cases.

Perilesional Bone Marrow Edema and Soft Tissue Swelling

In addition to the osseous changes discussed above, perilesional bone marrow edema and soft tissue abnormalities are also important indicators of infection in acute osteomyelitis cases. Furthermore, many other pathologic conditions can share these imaging appearances, thereby masquerading as an infectious disease and making accurate diagnosis difficult.

A B

Fig. 1. A 10-year-old female with osteosarcoma.
A. Proximal metaphysis of the right humerus shows "moth-eaten" and permeative bone destruction (arrows).
B. On contrast-enhanced T1-weighted MRI, strong enhancement of the soft tissue adjacent to the destructive bone lesion is evident, suggesting inflammation.

Here is a case of a 21-year-old male patient who had been complaining of right shoulder pain for several months although his shoulder joint appeared normal on the initial plain radiograph (Fig. 2A). However, MRI showed bone marrow edema on the coracoid process and inflammatory changes in adjacent soft tissues (Fig. 2B). After an initial diagnosis of acute osteomyelitis, the patient underwent surgery, after which the removed bony tissues were pathologically confirmed to be consistent with osteomyelitis. A year after the surgery, he had a follow-up MRI for persistent right shoulder pain. On follow-up MRI, a round, mass-like lesion was clearly visible at the base of the coracoid process. Meanwhile, reactive sclerosis and bone marrow edema had de-

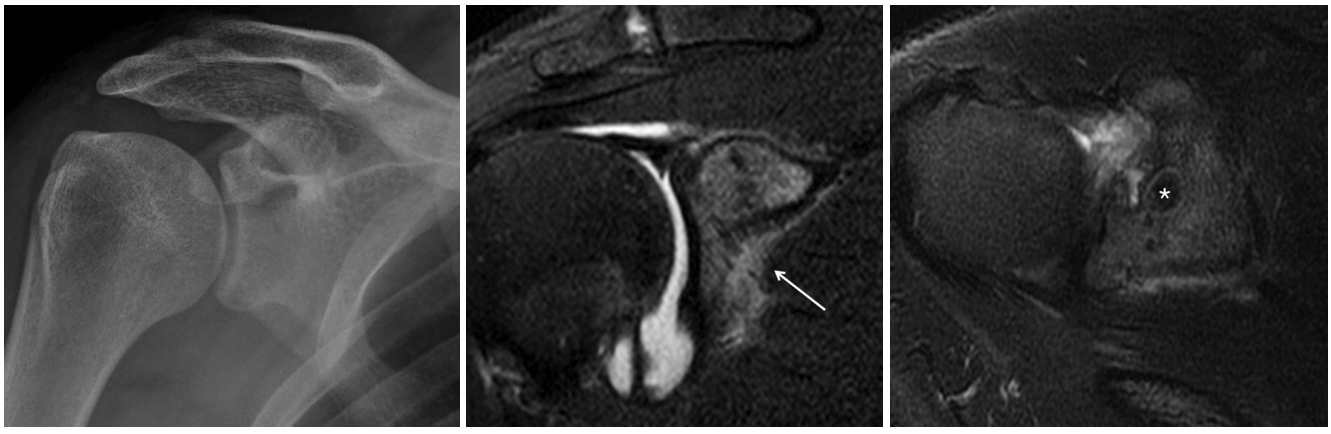

Fig. 2. A 21-year-old male with osteoid osteoma.
A. Plain radiograph of the right shoulder shows normal findings.
B. On coronal T2 fat suppression MRI, the high signal intensity of the coracoid process is indicative of bone marrow edema. Inflammatory changes of the adjacent soft tissues are also present (arrow).
C. Axial T2 fat suppression MRI taken one year later shows a well-circumscribed round mass-like lesion (asterisk) at the base of the coracoid process. It appears as a low signal intensity lesion with a high-signal-intensity peripheral rim. Reactive sclerosis and bone marrow edema have developed around the lesion.

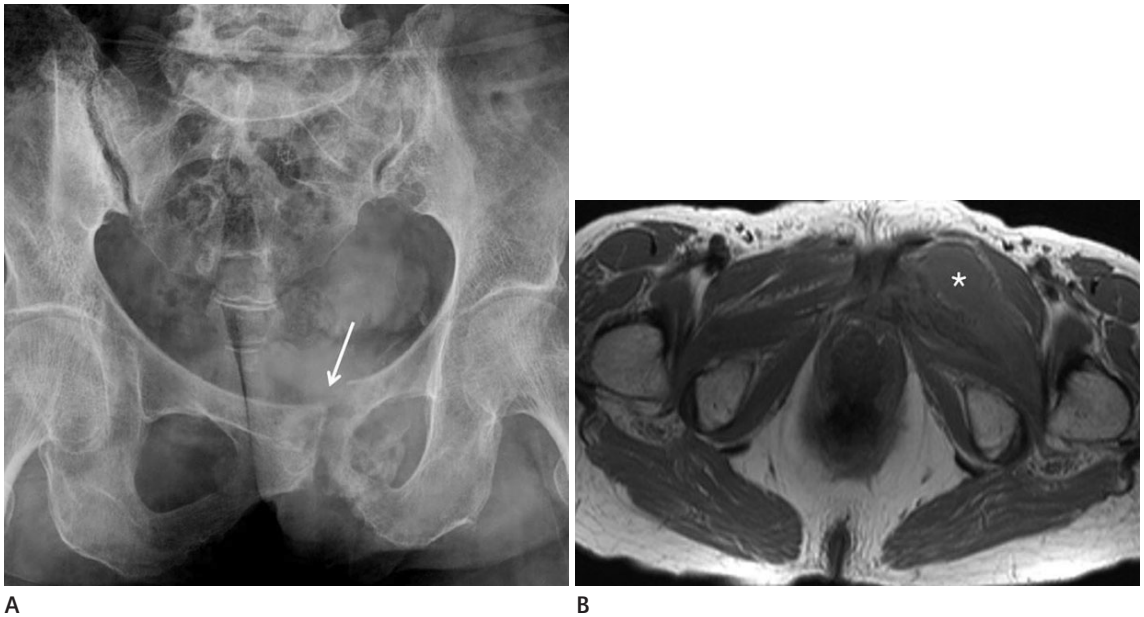

Fig. 3. A 65-year-old female with insufficiency fracture of the pelvis.
A. Plain radiograph of the pelvis shows a left pubic bone fracture (arrow) with reactive sclerosis and bone formation.
B. Axial contrast-enhanced MRI shows extensive perilesional bone marrow signal changes. Also, there is localized fluid collection that seems to be due to a hematoma (asterisk) near the fracture site. Such findings can easily be mistaken for an abscess pocket.

veloped around the new lesion (Fig. 2C). On a CT scan taken during the same period, an osteolytic lesion with a nidus was seen. The patient received a second surgery and the final pathologic diagnosis was osteoid osteoma.

In another case of a 65-year-old female patient, the plain radiograph of her pelvis showed a fractured left pubic bone along with several fractured fragments with irregular margins and reactive sclerosis (Fig. 3A). However, features observed on MRI appeared much more aggressive than expected from a simple insufficiency fracture. There were also perilesional marrow changes that were accompanied by fracture and hematoma, which could easily be confused with abscess formation (Fig. 3B). Such pelvic insufficiency fractures typically occur at the sacral ala and the parasymphyseal region of the os pubis (5). As seen in our case, fractures of the parasymphysis and pubic rami often have aggressive radiographic appearances, including increased lysis and bone fragments. Accompanying marrow edema and perilesional areas with increased signal intensity on MRI can increase the difficulty in selecting the correct diagnosis because such findings overlap with indirect signs of infection.

SUBACUTE OSTEOMYELITIS

Subacute osteomyelitis is a low-grade bone infection that occurs within 3 to 5 weeks of an initiating event. Various factors, such as increased host resistance, decreased bacterial virulence, and antibiotic administration contribute to an indolent course of subacute osteomyelitis. The most important manifestation of subacute osteomyelitis is a single focus of a geographic osteolytic lesion, known as the Brodie abscess, predominantly found in metaphyseal locations (6). Histopathologically, a Brodie abscess is walled off by reactive bone proliferation and the abscess cavity may contain pus, necrotic tissues, and pathogens. On plain radiographs, a Brodie abscess appears as a radiolucent lesion with or without sclerotic margins, whereas on MRI, it is typically seen as a well-demarcated collection of intraosseous fluid with peripheral enhancement. Below, we describe two very different conditions with similar radiographic appearances imitating a Brodie abscess.

A case of a 10-year-old male patient included a plain radiograph of his humerus that showed osteolytic lesions in the middle shaft (Fig. 4A). A periosteal reaction was observed on one

A B

Fig. 4. A 10-year-old male with Langerhan's cell histiocytosis.
A. Plain radiograph of the humerus shows a lobulated osteolytic lesion with periosteal reaction (arrow) at the mid shaft. There is no evidence of perilesional reactive sclerosis.
B. Contrast-enhanced MRI in the sagittal plane shows osteolytic lesions with adjacent cortical destruction and periosteal reaction (arrow). Swelling and enhancement of the surrounding soft tissues are also visible.

side but there was no definite evidence of reactive sclerosis. On MRI, cortical destruction, periosteal reaction, and swelling of the adjacent soft tissues were evident, supporting a suspected diagnosis of subacute osteomyelitis with an intraosseous abscess (Fig. 4B). However, the osteolytic lesion was finally confirmed to be Langerhan's cell histiocytosis (LCH). In the long bones, the imaging features of LCH can be correlated with the stage of the disease. On plain radiographs, LCH initially appears as ill-defined areas of bone destruction whereas in advanced stage, lesions develop well-defined margin with limited sclerosis (7). Also, smooth endosteal scalloping with a "budding appearance" on CT and MRI may be a useful imaging feature in diagnosis of LCH (8).

We observed another similar case of histiocytosis at a different location in a 19-year-old male patient's skull. On the axial CT scan, there was a well-defined osteolytic lesion with a geo-

graphic margin on the right parietal bone (Fig. 5A). Inside this hypodense osteolytic portion, there was an irregular bone density lesion, which is a typical feature of a devascularized bony fragment known as a sequestrum. The plain radiograph of the patient's skull showed similar findings, with no evidence of reactive sclerosis (Fig. 5B). Also, there was no significant periosteal reaction because the skull table usually does not undergo periosteal reaction. This patient underwent craniectomy of the

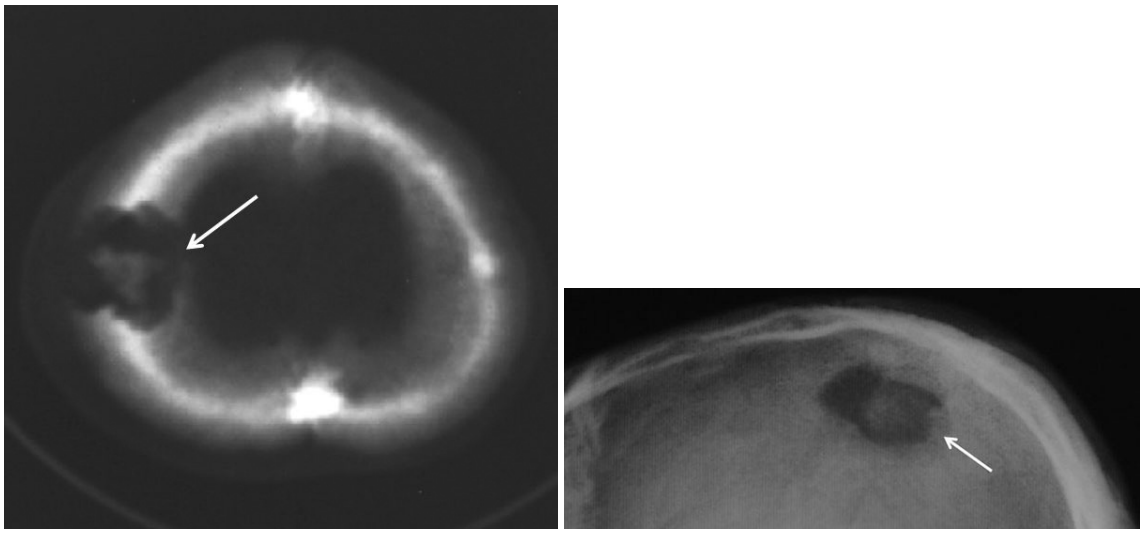

A B

Fig. 5. A 19-year-old male with Langerhan's cell histiocytosis.
A. An axial CT image of the skull shows an osteolytic lesion with a lobulated contour (arrow). At the center of the osteolytic lesion, there is a bony lesion with an irregular margin that is indicative of a sequestrum.
B. Similarly, the plain radiograph of the same patient's skull shows an osteolytic lesion (arrow) with an inner high-density portion. However, neither reactive sclerosis nor significant periosteal reactions are apparent near the osteolytic lesion.

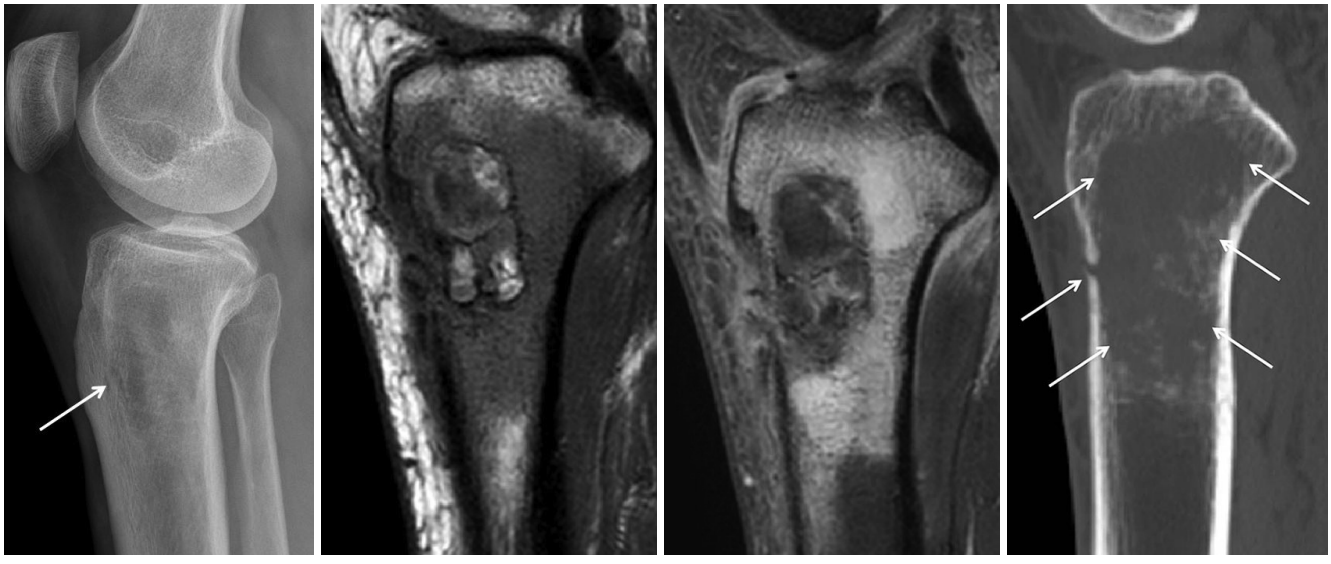

A B C D

Fig. 6. A 58-years-old female with fibroblastic osteosarcoma, grade IV.
A. Plain radiograph shows an ill-defined osteolytic bone lesion (arrow) accompanied by minimal sclerosis at the metaphysis of the left proximal tibia. There is no periosteal reaction.
B, C. On sagittal T1-weighted **(B)** and contrast-enhanced T1-spectral presaturation with inversion recovery MRI **(C)**, the bony destructive lesion has a lobulated contour with inner septa-like structures. There is an inner rim of intermediate to high signal intensity, and an outer rim of dark signal intensity.
D. CT image of the tibia shows more extensive bone destruction (arrows) than what was observed from MR images. Also, the low signal rim seen in MRI was not a bony sclerosis.

right parietal bone, after which the final pathologic diagnosis turned out to be an eosinophilic granuloma: a solitary, localized form of LCH confined to bone tissue (9).

Another malignant tumor mimicking a Brodie abscess by presenting with radiolucency on plain radiography is a variant of intramedullary osteosarcoma. The proximal tibia of a 58-year-old female patient showed an ill-defined, osteolytic bone lesion on plain radiograph. Minimal sclerosis can be seen on the metaphysis, but there was no periosteal reaction (Fig. 6A). Sagittal MRI of the same patient showed a well-defined bony destructive lesion at the anterior metaphysis of the proximal tibia. The destructive bony lesion has a lobulated contour with inner septa-like structures and there was also an inner rim of intermediate-to-high signal intensity, and an outer rim of dark signal intensity on T1-weighted MRI. Extensive reactive changes were evident at the bone marrow and the adjacent soft tissues (Fig. 6B, C). However, CT findings of the same lesion were somewhat different from MRI findings. More extensive bone destruction was apparent and the outer rim of low signal intensity was not a real bony sclerosis (Fig. 6D). After surgical excision, the final pathologic diagnosis was fibroblastic osteosarcoma, grade IV. Although the typical radiologic feature of an osteosarcoma is aggressive bone formation, purely osteolytic lesions do exist and account for approximately 10% of all cases (10). Such lesions can be observed in osteosarcoma subtypes, including fibroblastic, fibrohistiocytic, and giant-cell rich types (11).

CHRONIC OSTEOMYELITIS

The chronic osteomyelitis stage involves bone infections that persist for over 6 weeks despite appropriate treatment. Characteristic bony lesions at this stage include involucrum, sequestrum, and cloaca. An involucrum is new bone growth by the periosteum surrounding a sequestrum, which is a devascularized bone fragment (12). A cloaca is a defect in an involucrum through which purulent and necrotic materials escape. The best diagnostic clue for chronic osteomyelitis is thickened, irregular bone sclerosis, accompanied by periostitis. A progressive sclerosis develops around the areas of lytic bone destruction seen in the earlier disease stages. As the disease progresses with intermittent exacerbations, new areas of osteolysis, as well as periosteal reactions appear, resulting in sclerosis with associated hyperostosis (13).

A plain radiograph of a 73-year-old male patient's left lower extremity showed thickened and heterogeneously sclerotic bone at the tibial shaft (Fig. 7A). T1-weighted MRI showed diffuse thickening of the cortex with increased signal intensity. Also, changes in bone marrow signal intensity can be observed (Fig. 7B). The first diagnostic impression was chronic osteomyelitis

A B

Fig. 7. A 73-year-old male with bone metastasis.
A. Plain radiograph of the left lower extremity shows irregular cortical thickening with extensive sclerosis along the distal shaft of the tibia.
B. T1-weighted MRI in the coronal plane shows diffuse thickening of the cortex with increased signal intensity. Also, the bone marrow signal intensity is darker than normal (arrows).

of the tibial shaft. However, the chest CT scan of the same patient showed a cavitary lung mass that was later confirmed to be malignant. The bone scan taken for cancer work-up showed multifocal metastatic foci, including the ribs, sternum, pelvic bones, femurs, and tibia. Thus, the sclerotic bony lesion at the tibial shaft was in fact a metastatic lesion.

INFECTIOUS ARTHRITIS

Infectious arthritis, also known as septic arthritis, represents an invasion of the joint space by infectious organisms, such as bacteria or fungus. Being a hypervascular tissue without a basement membrane, the synovium is particularly vulnerable to bacterial invasion. Auto-digestion of the joint cartilage occurs by various proteinases, cytokines, and reactive oxygen species produced from reactions between the causative agent and the host's synovial and cartilaginous tissues. The infection of synovial or periarticular tissues produces various clinical symptoms, such as joint pain and swelling, effusion, and decreased range of motion. The first detectable radiographic sign of infectious arthritis is joint effusion, followed by joint space narrowing and cortical bone destruction. Diffuse periarticular bone marrow enhancement can also be seen. The following three cases demonstrate such findings.

On the initial plain radiograph of an 80-year-old female patient's right shoulder, only mild degenerative changes without significant joint space narrowing were observed. Yet during the course of the following 8 months, rapid progression in the destruction of articular margins followed resulting in a markedly reduced joint space with multifocal detached osseous fragments (Fig. 8A, B). MRI of her shoulder showed severe narrowing of the joint space with destruction of the subchondral bone. Also, a large amount of effusion with fluid signal intensity was seen to cause capsular distension in her shoulder joint. After contrast enhancement, the joint capsule as well as the subchondral portion adjacent to the destroyed articular bone showed diffuse enhancement, although periarticular soft tissue changes were not prominent (Fig. 8C). Unlike the initially suspected diagnosis of infectious arthritis, this patient was diagnosed with neurotrophic arthritis. Often, radiologists face a major dilemma when attempting to distinguish neurotrophic arthritis from bone infections, such as septic arthritis, because the radiographic findings overlap substantially. An additional diagnostic challenge is found when a bone infection is superimposed on top of underlying neurotrophic arthropathy (14). Neurotrophic, as well as infectious joints, both have an extremely rapid course of bone destruction with a large amount of joint effusion and bony enhancement. However, fluid collections in infectious joints may contain less prominent osseous debris compared with neurotrophic arthropathy.

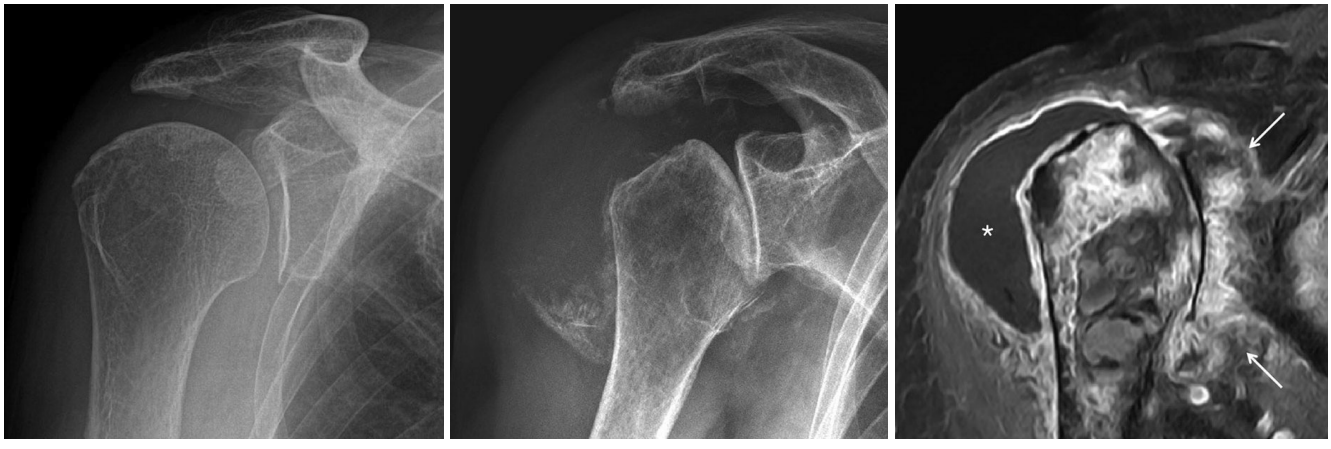

A B C

Fig. 8. An 80-year-old female with neurotrophic arthropathy.
A. Plain radiograph of the patient's right shoulder shows only mild degenerative changes without joint space narrowing.
B. After 8 months, her right shoulder joint shows rapid destruction of its articular margins. Multifocal detached osseous fragments are visible.
C. Contrast-enhanced T1-spectral presaturation with inversion recovery MRI in the coronal plane shows diffuse enhancement along the subchondral portion and the joint capsule (arrows). Also, capsular distension caused by a large amount of effusion (asterisk) can be seen. However, periarticular soft tissue changes are not prominent.

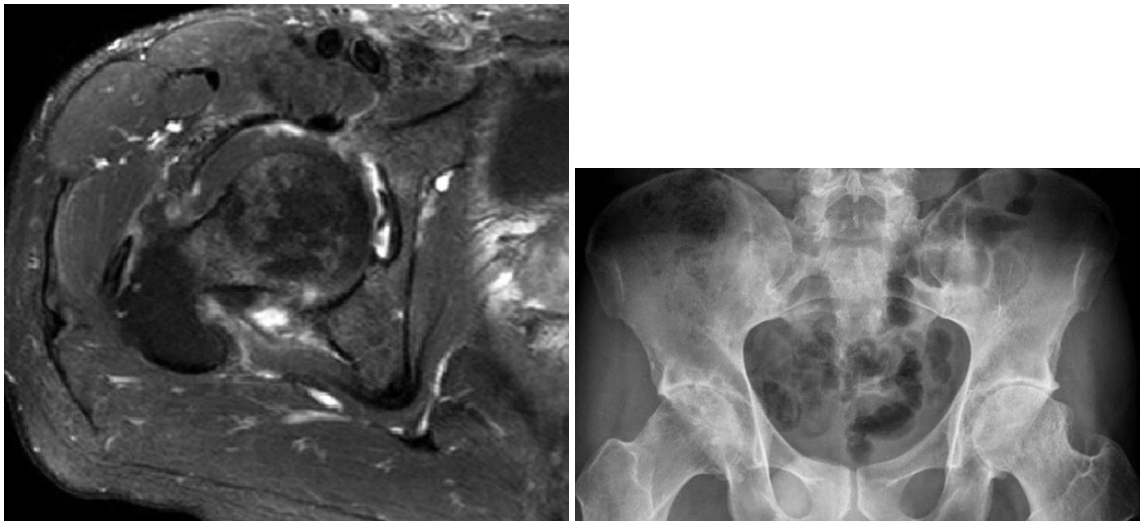

A B

Fig. 9. A 35-year-old male with ankylosing spondylitis involvement of hip joints.
A. Axial contrast-enhanced T1-spectral presaturation with inversion recovery MRI of the right hip joint shows periarticular soft tissue edema. Joint effusion with capsular distension and the narrowing of the joint space are also evident. However, there are no significant signal changes in the bony structures.
B. Plain radiograph of the pelvis in the same patient shows complete ankylosis of both sacroiliac joints. This patient has an underlying ankylosing spondylitis with involvement of both hip joints.

The second case mimicking infectious arthritis was a 35-year-old male patient's right hip joint, accompanied by joint effusion with a distended joint capsule that was evident on MRI. Also, significant narrowing of the joint space and subchondral bone erosion were observed. Periarticular soft tissue edema was present on the contrast-enhanced MRI, but there was no significant signal change in the bony structures (Fig. 9A). Considering such radiographic appearances, the initial diagnostic impression was septic arthritis of the hip joint. However, on the plain radiograph of the same patient's pelvis, bilateral hip joint space narrowing with axial migration of femoral heads and a collar of osteophytes at the femoral head-neck junction suggest that he has an underlying ankylosing spondylitis (Fig. 9B). In fact, the lesions observed in his right hip joint did not result from a septic condition. Along with the sacroiliac joints, his right hip joint was also being invaded by ankylosing spondylitis. Ankylosing spondylitis is a chronic inflammatory arthropathy that primarily affects the axial skeleton. The prevalence of hip involvement in patients with ankylosing spondylitis is relatively high, being reported in approximately 24–36% of patients (15). Unlike syndesmophyte formation in the vertebral columns, synovial inflammation within the involved peripheral joints, such as hips and shoulders, causes cartilage loss and bone erosion, thereby resulting in narrowing of the joint space (16).

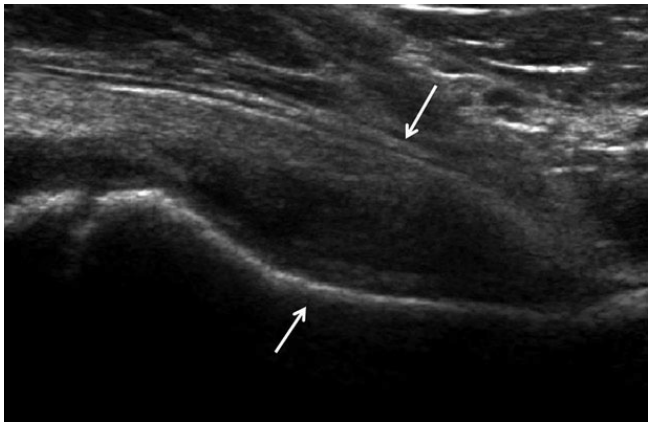

Fig. 10. An 8-year-old female with transient synovitis of the hip. Ultrasound findings of the right hip joint include joint effusion with synovial hypertrophy and capsular distention (arrows). However, the capsular margin is well preserved and there are few pericapsular changes.

In another case, the hip joint of an 8-year-old female patient showed joint effusion with synovial hypertrophy and capsular distension on ultrasonography (Fig. 10). Similar radiographic findings can be observed in cases with Legg-Calve-Perthes disease and septic arthritis. However, the margin of this patient's hip joint capsule was relatively well-defined with scarce pericapsular changes. Considering that septic arthritis normally

presents with indistinct capsular margins and prominent pericapsular inflammatory changes, the absence of such appearances could be an indicator that septic conditions can be excluded from the candidate diagnoses, in favor of less aggressive conditions, such as a transient synovitis of the hip.

INFECTIOUS SPONDYLITIS

A spinal infection can occur via various contamination routes. Most commonly, infectious organisms can be lodged in the bone marrow of the vertebrae via hematogenous spread. Other sources of infection include a direct spread from contiguous septic foci, postoperative infection, or penetrating trauma (17). Along with clinical manifestations and laboratory data, imaging plays an important role in localization and characterization of vertebral and intervertebral disc infections.

Loss of Intervertebral Disc Space, Paravertebral Masses and Abscess Formation

The early abnormalities of infectious spondylitis are rapid reduction in intervertebral disc height accompanied by subchondral bone erosion at adjacent endplates. Involvement of at least two consecutive vertebrae is typical because the infection spreads through the intervening disc space. Identification of paravertebral soft tissue masses and abscesses is also indicative of the infectious nature of the condition.

The plain radiograph of a 68-year-old male patient's T-L spine showed bony ankylosis of the T11 and T12 vertebral bodies (Fig. 11A), which is a frequently observed sequelae of infectious spondylitis. On sagittal views of T1-weighted MRI, the body heights of T11 and T12 vertebrae appeared decreased, accompanied by partial bony ankylosis. There were also fat marrow signal changes at the right lateral portions and the pedicles of the concerned vertebrae, and a paravertebral mass formation was evident on the right side (Fig. 11B). CT-guided aspiration of this paravertebral mass was performed using an 18-G biopsy needle, and the pathologic diagnosis was metastatic adenocarcinoma.

Another case of a 73-year-old male patient's cervical spine also presented with confusing radiographic findings. On the plain radiograph, a collapsed C5 vertebral body was visible with anterior displacement upon C6 (Fig. 12A). On an MRI taken for

A B

Fig. 11. A 68-year-old male with vertebral metastasis.
A. Plain radiograph of T-L spine in the lateral view shows bony ankylosis at the T10-T12 levels. This finding is suggestive of sequelae of infectious spondylitis.
B. Sagittal T1-weighted MRI shows decreased body heights of T11 and T12 as well as partial ankylosis. The right lateral portions and the pedicles are seen as low signal intensity and there is also a paravertebral mass formation on the right side.

further evaluation, the collapsed C5 with marrow signal changes seemed to be a result of a pathologic compression fracture. An epidural mass formation at the same level was also detected, which supported the initial diagnosis of metastasis (Fig. 12B). However, the same patient's CT image showed osteolytic bone destruction predominantly confined to the central portion of the vertebral body and reactive sclerosis on the remaining uninvolved bones (Fig. 12C). Such findings raised the possibility of this disease being an infectious one, and considering the relatively less noticeable inflammatory changes in the adjacent soft tissue, tuberculous spondylitis seemed an appropriate diagnosis for this patient's condition. However, the final diagnosis was consistent with the initial presumptive impression: bony metastasis.

Differentiating vertebral metastasis from infectious spondylitis is crucial because their therapeutic managements are significantly different. On MRI, spinal metastasis is more likely to involve non-contiguous vertebrae, causing a more aggressive destruction

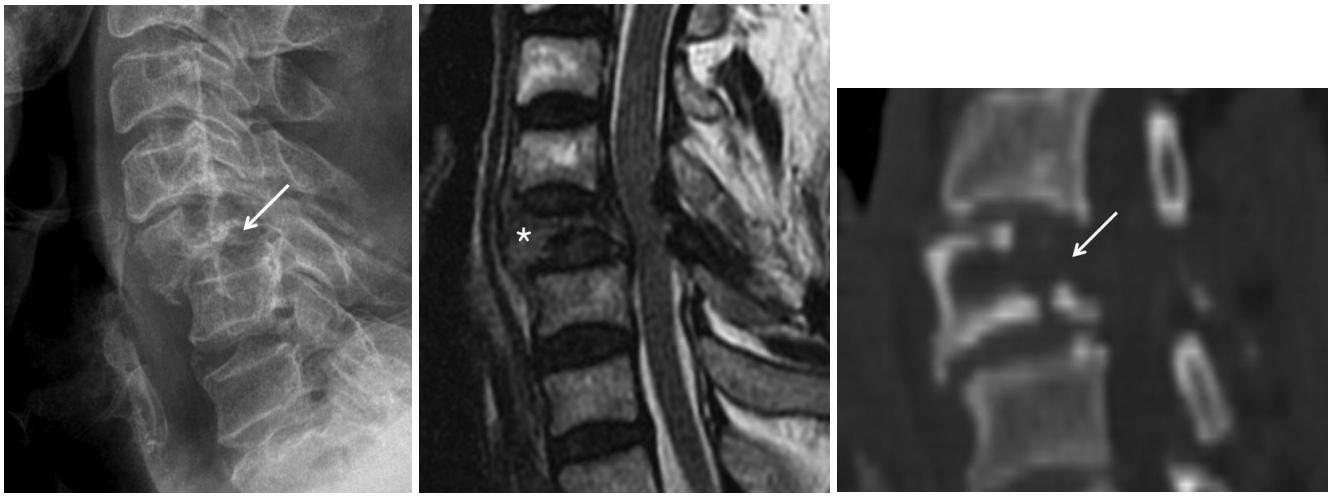

A B C

Fig. 12. A 73-year-old male with vertebral metastasis.
A. Plain radiograph of the C-spine in the lateral view shows a collapsed C5 body with severe anterolisthesis upon C6 (arrow).
B. Sagittal T2-weighted MRI of the C-spine shows a pathologic compression fracture at the C5 body (asterisk) as well as an epidural mass formation.
C. Sagittal CT image of the same patient shows osteolytic bone destruction with reactive sclerosis on the remaining bones (arrow). Such findings may be seen in infectious lesions like tuberculosis.

of vertebral bodies and endplates with overt paravertebral soft tissue mass formation when compared with infectious spondylitis (18). Moreover, a decrease in height of the involved vertebral bodies is a common finding despite the fact that the intervertebral disc space is usually preserved in spinal metastasis (19).

Sclerosis or Eburnation

As infectious spondylitis progresses, regenerative changes take place and reactive sclerosis or eburnation of vertebral endplates may subsequently appear. Such osteosclerotic responses are typically more prominent in pyogenic spondylitis, but they can also be seen in tuberculous types.

A 60-year-old male patient's L-spine MRI showed severe disc degeneration at the L5-S1 level with subchondral bone erosion at the adjacent endplates. Disc extrusion was evident (Fig. 13A). On the CT scans of the same patient, secondary reactive sclerosis at the endplates of L5 and S1 seemed very prominent, accompanied by vacuum phenomenon features (Fig. 13B). Such nonspecific findings can be easily observed in the late stages of infectious spondylitis. However, the underlying mechanism of bone destruction is very different between the two disease entities. During the course of degeneration, bone destruction can result from continuous mechanical forces, such as abrasion. However, similar results can be obtained through the osteolysis process caused by infection.

A B

Fig. 13. A 60-year-old male with degenerative changes of L-spine.
A. Sagittal T2-weighted MRI of the L-spine shows severe disc degeneration with bone erosion (arrow) caused by mechanical forces at L5-S1.
B. Sagittal CT image of the same patient shows disc herniation at L5-S1, with secondary sclerotic changes in the adjacent vertebral bodies.

CONCLUSION

Infectious diseases of the MSK system share many radiographic findings with various other disease entities. An awareness of potential infection mimics is helpful to avoid diagnostic errors, which could lead to catastrophic results for the patient.

REFERENCES

1. Poultsides LA, Liaropoulos LL, Malizos KN. The socioeconomic impact of musculoskeletal infections. *J Bone Joint Surg Am* 2010;92:e13
2. Manaster BJ. *Diagnostic imaging: musculoskeletal non-traumatic disease*. Philadelphia, PA: Elsevier Health Sciences 2016
3. Resnick D. *Osteomyelitis, septic arthritis, and soft tissue infection: organisms*. In Resnick D, ed. *Bone and Joint Imaging*. Philadelphia, PA: Saunders 1989:753-788.
4. Pineda C, Espinosa R, Pena A. Radiographic imaging in osteomyelitis: the role of plain radiography, computed tomography, ultrasonography, magnetic resonance imaging, and scintigraphy. *Semin Plast Surg* 2009;23:80-89
5. Peh WC, Khong PL, Yin Y, Ho WY, Evans NS, Gilula LA, et al. Imaging of pelvic insufficiency fractures. *Radiographics* 1996;16:335-348
6. Hayes CS, Heinrich SD, Craver R, MacEwen GD. Subacute osteomyelitis. *Orthopedics* 1990;13:363-366
7. Mhuircheartaigh JN, Lin YC, Wu JS. Bone tumor mimickers: a pictorial essay. *Indian J Radiol Imaging* 2014;24:225-236
8. Khung S, Budzik JF, Amzallag-Bellenger E, Lambilliote A, Soto Ares G, Cotten A, et al. Skeletal involvement in Langerhans cell histiocytosis. *Insights Imaging* 2013;4:569-579
9. Kaul R, Gupta N, Gupta S, Gupta M. Eosinophilic granuloma of skull bone. *J Cytol* 2009;26:156-157
10. Joo I, Choi JA, Chung JH, Oh JH, Hong SH, Kang HS. Fibroblastic type osteosarcoma of the ulna: a case report of a tumor in a rare location with atypical imaging findings. *Korean J Radiol* 2009;10:85-88
11. Sundaram M, Totty WG, Kyriakos M, McDonald DJ, Merkel K. Imaging findings in pseudocystic osteosarcoma. *AJR Am J Roentgenol* 2001;176:783-788
12. Perron AD, Brady WJ, Miller MD. Orthopedic pitfalls in the ED: osteomyelitis. *Am J Emerg Med* 2003;21:61-67
13. Khanna G, Sato TSP, Ferguson P. Imaging of chronic recurrent multifocal osteomyelitis. *Radiographics* 2009;29:1159-1177
14. Giurato L, Uccioli L. The diabetic foot: Charcot joint and osteomyelitis. *Nucl Med Commun* 2006;27:745-749
15. Vander Cruyssen B, Muñoz-Gomariz E, Font P, Mulero J, de Vlam K, Boonen A, et al.; ASPECT-REGISPONSER-RESPONDIA working group. Hip involvement in ankylosing spondylitis: epidemiology and risk factors associated with hip replacement surgery. *Rheumatology (Oxford)* 2010;49:73-81
16. Jeong H, Eun YH, Kim IY, Kim H, Lee J, Koh EM, et al. Characteristics of hip involvement in patients with ankylosing spondylitis in Korea. *Korean J Intern Med* 2017;32:158-164
17. Hong SH, Choi JY, Lee JW, Kim NR, Choi JA, Kang HS. MR imaging assessment of the spine: infection or an imitation? *Radiographics* 2009;29:599-612
18. Shah LM, Salzman KL. Imaging of spinal metastatic disease. *Int J Surg Oncol* 2011;2011:769753
19. Khattry N, Thulkar S, Das A, Khan SA, Bakhshi S. Spinal tuberculosis mimicking malignancy: atypical imaging features. *Indian J Pediatr* 2007;74:297-298

근골격계 감염과 유사한 질환들: 임상 화보

강혜진[1] · 최희영[1] · 박지선[1] · 박소영[2] · 진 욱[2] · 류경남[1]*

골수염, 감염성 관절염 및 척추염과 같은 근골격계 감염은 발생 원인 및 임상 감염 단계에 따라 다양한 영상의학적 소견을 보인다. 그러나 근골격계 감염과 유사한 영상 소견을 보이지만 감염의 증거가 없는 다른 질환들도 존재하며, 이들은 단순 퇴행성 병변에서부터 골 종양에 이르기까지 다양하다. 따라서 근골격계 감염성 질환에서 전형적으로 나타나는 영상의학적 특징들을 접하였을 때 근골격계 감염과 유사한 비감염성 근골격계 질환의 가능성도 함께 고려하는 것이 중요하다.

[1]경희대학교 의과대학 경희대학교병원 영상의학과, [2]경희대학교 의과대학 강동경희대학교병원 영상의학과